JACS
JOURNAL OF THE AMERICAN CHEMICAL SOCIETY
Article
pubs.acs.org/JACS

Mechanistic Insight into the Superoxide Induced Ring Opening in Propylene Carbonate Based Electrolytes using in Situ Surface-Enhanced Infrared Spectroscopy

J. Padmanabhan Vivek,[†] Neil Berry,[†] Georgios Papageorgiou,[‡] Richard J. Nichols,[†] and Laurence J. Hardwick*[,†]

[†]Department of Chemistry, University of Liverpool, Liverpool L69 7ZD, United Kingdom
[‡]Department of Physics, University of Liverpool, Liverpool L69 7ZF, United Kingdom

Supporting Information

ABSTRACT: Understanding the mechanistic details of the superoxide induced solvent degradation, is important in the development of stable electrolytes for lithium−oxygen (Li—O_2) batteries. Propylene carbonate (PC) decomposition on a model electrode surface is studied here using in situ attenuated total reflectance surface enhanced infrared absorption spectroscopy (ATR-SEIRAS). The sensitivity of the SEIRAS technique to the interfacial region allows investigation of subtle changes in the interface region during electrochemical reactions. Our SEIRAS studies show that the superoxide induced ring opening reaction of PC is determined by the electrolyte cation. Computational modeling of the proposed reaction pathway of superoxide with PC revealed a large difference in the activation energy barriers when Li^+ was the countercation compared with tetraethylammonium (TEA^+), due to the coordination of Li^+ to the carbonate functionality. While the degradation of cyclic organic carbonates during the Li—O_2 battery discharge process is a well-established case, understanding these details are of significant importance toward a rational selection of the Li—O_2 battery electrolytes; our work signifies the use of SEIRAS technique in this direction.

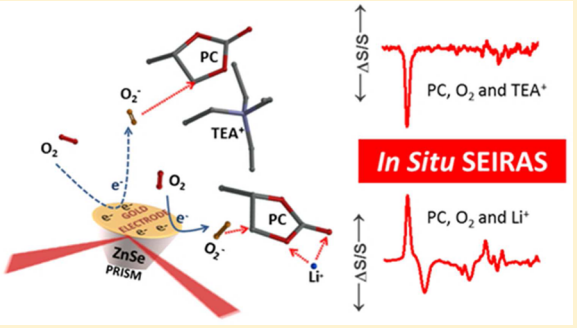

INTRODUCTION

Lithium−oxygen (Li—O_2) batteries have attracted a great deal of research interest in recent years for their promising specific energy.[1−9] The electrolytes used in nonaqueous lithium based batteries are primarily mixtures of aprotic organic solvents and lithium salts, the major prerequisite characteristics of the solvents being lithium transport properties (ionic conductivity) and electrochemical stability (wide electrochemical window). There is a growing interest in the fundamental aspects of electrode processes in nonaqueous electrolytes because of their wide application in these battery systems. The physical properties of the electrolytes such as viscosity, Li-ion solubility, oxygen solubility, electrode wettability and thermal stability also determine the performance of a battery. Organic carbonate based electrolytes have been a popular choice for Li-ion batteries[10−13] because of their wide electrochemical window and good compatibility with conventional lithium battery electrodes. Organic carbonates have also been tested for Li—O_2 cells, but have been found unsuitable because of their instability in the presence of reduced oxygen species.[5,14−16] Although the degradation of cyclic organic carbonates used in Li—O_2 battery systems has already been demonstrated,[14] the mechanism of the electrolyte decomposition at the electrode/electrolyte interface is not clearly defined; this is largely because of the difficulty in investigating the electrode interfaces while these reactions are happening inside the battery. A mechanistic understanding of these reactions at the metal/electrolyte interface is a key step in controlling and eliminating the side reactions affecting the performance of the battery.

In spite of the adequate stability of organic carbonate electrolytes in Li-ion battery systems; their degradation in Li—O_2 batteries is believed to be due to the nucleophilic attack of reduced oxygen species, primarily superoxide, generated at the cathode.[2,14,17−19] Although the degradation products of cyclic organic carbonates such as propylene carbonate (PC) and ethylene carbonate (EC) have been well studied on the Li—O_2 cathode by ex situ methods, the proposed reaction mechanisms remain speculative. Because of the challenges in tracing the reaction products and intermediates as they are formed at the interface of battery electrodes, the reaction mechanisms are generally supported by theoretical predictions. Numerous quantum chemical studies have been reported in recent years on the reductive decomposition of cyclic organic carbonates such as EC and PC,[12,20−22] which consider different reaction pathways of a nucleophile induced decomposition of these solvent molecules. Since these theoretical studies cannot afford the complexities of a real battery electrolyte system, supporting

Received: November 30, 2015
Published: February 24, 2016

DOI: 10.1021/jacs.5b12494
J. Am. Chem. Soc. 2016, 138, 3745−3751

empirical evidence from model systems is preferred. In situ spectroelectrochemistry studies are promising in this direction; in situ infrared spectroscopy has been employed for studying battery electrolytes by various research groups in the recent years.[23,24] In this direction, attenuated total reflection surface enhanced infrared spectroscopy (ATR-SEIRAS) can offer a rather detailed in situ analysis of the interfacial region. The advantage of this internal reflection technique pioneered by Osawa and co-workers,[25] is its sensitivity to the interfacial region (ca. within 10 nm from the electrode surface) because of the surface enhancement afforded by the thin gold film electrode as well as the reduction of the bulk electrolyte signal as the infrared beam does not pass through the electrolyte. The evanescent wave propagating along the dielectric interface decays exponentially from the surface, thus discriminating the interfacial region from the bulk electrolyte.

We report an in situ electrochemical ATR-SEIRAS study on the reactivity of PC at a noble metal electrode interface (gold) in an attempt to evaluate the proposed noncatalytic path of superoxide induced decomposition of PC. The primary objective of these measurements has been to study the Au/PC-$LiClO_4$ electrochemical interface in oxygen saturated as well as deoxygenated conditions. Further, in order to elucidate the role of lithium in determining the reactions at the interface, SEIRA spectra with electrolytes containing tetraalkylammonium salt, in place of lithium salt, were also recorded. A dramatic difference in the stability of propylene carbonate has been observed between these two systems. Our computational studies revealed that the interactions of the propylene carbonate oxygen atoms with the Li^+ cations are crucial in determining the stability of this molecule in the presence of superoxide.

EXPERIMENTAL SECTION

A schematic view of the SEIRA spectroelectrochemical cell is shown in Figure 1. The spectroelectrochemical cell was formed by a Teflon

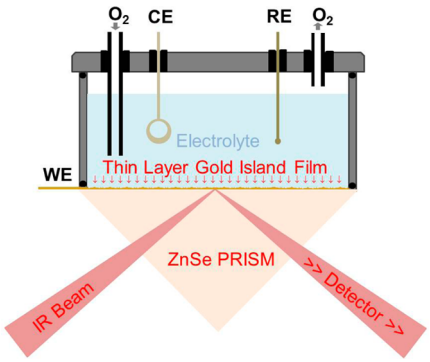

Figure 1. Schematic of SEIRA spectroelectrochemical cell.

liquid cup attached on top of an internal reflection element (IRE), ZnSe. This ZnSe IRE spectroelectrochemical cell eliminates the large absorption in the lower wavenumber region compared to original Si IRE spectroelectrochemical cells. The ZnSe prism used as the ATR element was polished, thoroughly cleaned in deionized water, sonicated in ethanol, and then dried. The working electrode was a 15 nm thick Au film deposited on the polished surface of a ZnSe prism by thermal evaporation.[26,27] Electrochemical measurements were performed using Bio-Logic potentiostat. A coiled Pt wire was used as the counter electrode and a polished silver wire as the reference electrode; the reference potentials were then adjusted to the Li/Li^+ couple for convenience.

Electrolytes were prepared by mixing anhydrous HPLC grade PC (distilled then dried over activated 4 Å molecular sieves) with either tetraethylammonium perchlorate ($TEAClO_4$) or lithium perchlorate ($LiClO_4$) salt. The ATR-SEIRAS cell components and the perchlorate salts were dried at 120 °C under vacuum for 12 h. *Caution: Organic perchlorates and perchlorate salts of metal ion complexes are potentially explosive and should be treated with great care.* All solutions were prepared inside an argon-filled glovebox and electrolytes were purged using dry argon or oxygen inside the glovebox. The water content was measured using a Karl Fisher KF Coulometer (Metrohm); typically the electrolyte contained less than 10 ppm water. The sealed electrochemical cell was brought outside the glovebox for in situ SEIRAS measurements.

The ATR-FTIR measurements were conducted at room temperature with a Bruker IFS66v spectrometer equipped with MCT detector. The angle of incidence was set at 65°, and the spectral acquisition was conducted using p-polarized infrared radiation at 4 cm^{-1} resolution. The interferometer was driven by dry air, and the specular reflection assembly was also purged with dry air (CO_2 free). The electrode potential was varied from the open circuit potential to the oxygen reduction region then reversed toward respective positive potentials. Spectra were collected at varying potentials by holding the potentials while collecting the spectral signals for 30 s at 4 cm^{-1} resolution. SEIRA spectra were plotted as the relative change in the IR signal at the voltage of interest with respect to the open circuit voltage (OCV) using the formula:

$$\frac{\Delta S}{S} = \frac{S_{\text{variable}} - S_{\text{OCV}}}{S_{\text{OCV}}} \quad (1)$$

In this format, a negative going peak in the spectra indicates an increase in absorbance at the corresponding wavenumber.

Computational Methods. All stationary points were fully optimized with Gaussian 09[28] using M06-2*X*/6-311++(d.p).[29] An ultrafine grid density was used for numerical integration in all DFT calculations. Harmonic vibrational frequencies were computed for all optimized structures to verify that they were either minima or transition states, possessing zero imaginary frequencies and one imaginary frequency, respectively. Calculations were performed with M06-2X functional, which is constructed to include nonlocal effects of electronic dispersion and is found to give good estimates for reaction enthalpies in bond-forming reactions. Coordinates of the species calculated can be found in the Supporting Information (SI).

RESULTS AND DISCUSSION

Figure 2a shows cyclic voltammograms on a Au thin film electrode at 0.1 V/s scan rate in the typical ORR/OER potential region, recorded in deoxygenated as well as oxygen saturated 0.1 M $TEAClO_4$/PC electrolyte. The voltammogram of the deoxygenated electrolyte shows no faradaic current, indicating a stable potential window; a negative going current peak seen in oxygenated electrolyte (red) indicates reduction of oxygen. The reduced oxygen species (presumably superoxide) does not appear to be reoxidizable as only a very small anodic peak is observed at this scan rate. The tetraalkylammonium cation generally stabilizes the superoxide anion, enabling the latter to be reoxidized during the reverse potential sweep; ORR in electrolytes comprising tetraalkylammonium salts and relatively stable solvents such as acetonitrile and dimethyl sulfoxide are known to be pseudoreversible.[16]

The irreversibility of oxygen reduction in PC containing electrolytes indicates the instability of superoxide in this solvent. It is generally understood that O_2^- preferentially attacks the less hindered ethereal carbon of cyclic carbonates, leading to a ring opening reaction (Scheme 1). Interestingly, the anodic peak corresponding to the oxidation of superoxide in PC/$TEAClO_4$ is stronger and the superoxide formed shows

DOI: 10.1021/jacs.5b12494
J. Am. Chem. Soc. 2016, 138, 3745−3751

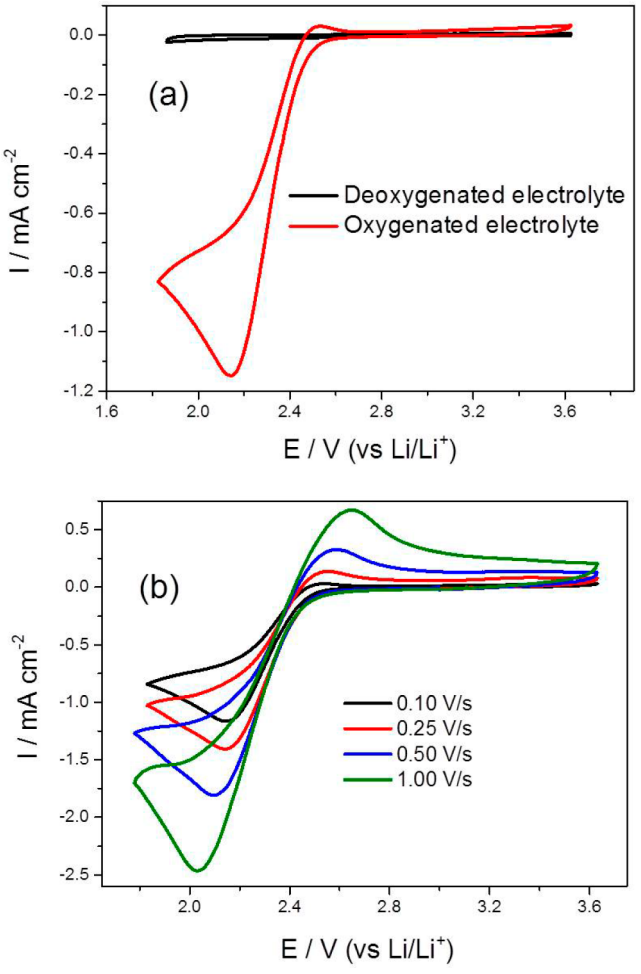

Figure 2. Cyclic voltammograms (a) the reduction of oxygen (red) and the argon background (black) in 0.1 M $TEAClO_4$/PC, at 0.1 V/s scan rate. (b) for the oxygen reduction reaction in 0.1 M $TEAClO_4$/PC, at 4 different scan rates.

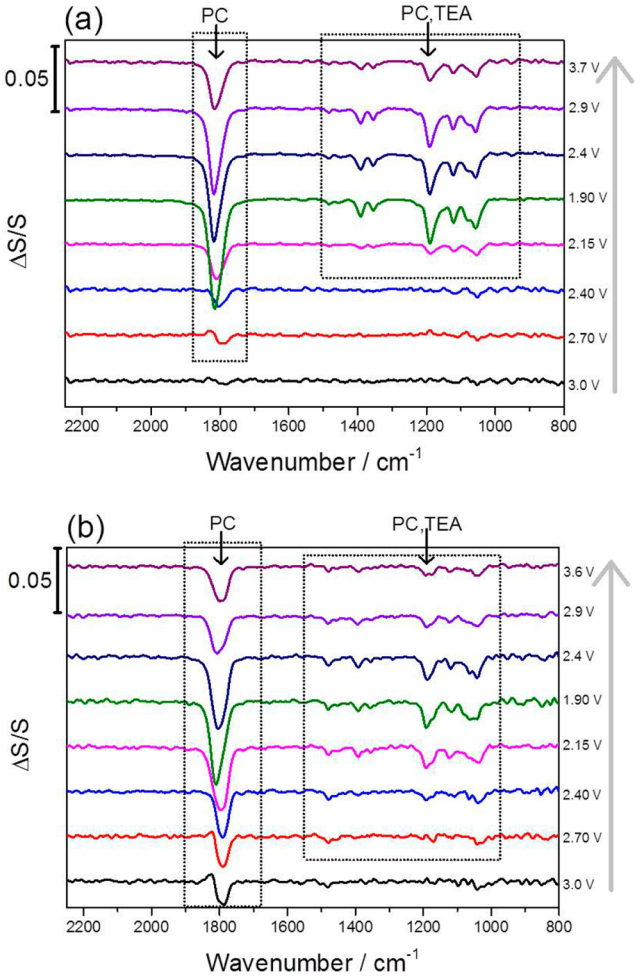

Figure 3. SEIRA spectra recorded for a Au thin film electrode in 0.1 M $TEAClO_4$/PC electrolyte at various representative electrode potentials. (a) Deoxygenated electrolyte—corresponds to the black CV curve in Figure 2a, and (b) oxygen saturated electrolyte—corresponds to the red CV curve in Figure 2a. The reference spectra were taken at open circuit voltage (3.3 V) before the potential sweep started.

Scheme 1. Superoxide Induced Ring Opening in PC

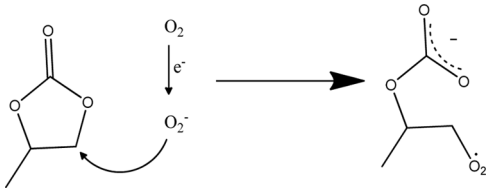

more reversibly behavior at higher scan rates (Figure 2b). This implies that the superoxide generated at the interface is stable only for a short period.

SEIRA spectra in Figure 3a correspond to the voltammogram in deoxygenated electrolyte (Figure 2a, corresponding spectra over a broader range is provided in the SI Figure S1), and these show growing downward-pointing peaks as the electrode potential is made more negative. All these bands resemble typical PC bands, but a shift in the C═O stretch to higher wavenumber is observed as the electrode potential is moved toward more negative values. As shown in Table 1, there is a 16 cm^{-1} shift in the C═O stretch of PC, on changing the potential from 3.0 to 1.9 V. This shift may indicate a stronger intermolecular dipole−dipole interactions or surface−dipole interactions as a result of selective partitioning or orientation of PC at the interface at these potentials. Apart from the PC and TEA vibrational bands, no new peaks are observed in this case, indicating that no new species (detectable within this spectral range) are formed at the interface. SEIRAS in Figure 3b corresponds to oxygenated electrolyte, showing very similar features, including the shift (25 cm^{-1}) in carbonyl stretch, as in the deoxygenated system. SEIRAS bands of both oxygenated and deoxygenated PC-$TEAClO_4$ systems at three representative potentials (as the potential is scanned from OCV through 3.0 to 1.90 V, then reversed the scan toward 3.6 V) are listed in Table 1. It is rather surprising that even though oxygen reduction is quasireversible, SEIRAS analysis does not indicate any superoxide induced reaction products in the interfacial region; for instance, the ring-opened reaction products of PC. While parasitic chemical reactions happening in the bulk electrolyte (away from the interfacial region) will not be observed in SEIRA spectra, our results indicate that no appreciable superoxide induced degradation of PC directly at the interface happens under these conditions.

The presence of ring-opened reaction products of cyclic organic carbonate based electrolytes in both Li-ion battery anode as well as Li—O_2 cathodes have been extensively

DOI: 10.1021/jacs.5b12494
J. Am. Chem. Soc. 2016, 138, 3745−3751

Table 1. SEIRAS Band Assignments of PC-TEAClO$_4$

	bands (cm^{-1}) at representative potentials			assignment[b]	
	3.0 V	1.90 V	3.6 V	vibration	species
PC-TEAClO$_4$/Argon	1801	1817	1815	ν(C═O)	PC
		1482	1482	$\tau(CH_2)$ + $\zeta(CH_2)$	PC, TEA
		1391, 1355	1398, 1355	$\delta(CH_3)$,ν_{ring}, $\omega(CH_2)$, ω(O—CH_2)	PC, TEA
		1190, 1122	1190, 1122	ν_s(C—O—C)+ ν_{as}(O—C—O), ν_s(CH_2—CH—CH_3)	PC
	1051	1057	1057	ν_s(C—O), ν_s(C—CH_3)	PC
PC-TEAClO$_4$/Oxygen	1788	1813	1800	ν(C═O)	PC
	1480	1480	1480	$\tau(CH_2)$ + $\zeta(CH_2)$	PC, TEA
	1391	1391, 1355	1391, 1355	$\delta(CH_3)$, ν_{ring}, $\omega(CH_2)$, ω(O—CH_2)	PC, TEA
		1191, 1118	1192, 1123	ν_s(C—O—C)+ ν_{as}(O—C—O), ν_s(CH_2—CH—CH_3)	PC
		1064, 1041	1041	ν_s(C—O), ν_s(C—O), ν_s(C—CH_3)	PC
	bands (cm^{-1}) at representative potentials			assignment[b]	
	2.12 V		3.7 V	vibration	species
PC-LiClO$_4$/Argon	1803		1817	ν(C═O)	PC
PC-LiClO$_4$/Oxygen	1813(+)[c]		1813(+)	ν(C═O)	PC
	1676		1676	ν(C═O)	$ROCO_2Li$
	1401		1401	$\omega(CH_2)$ + ω(O—CH_2)	$ROCO_2Li$
	1375		1375	$\delta(CH_3)$	$ROCO_2Li$
	1315		1315	$\tau(CH_2)$	$ROCO_2Li$
	1094		1093	(unassigned)	
	1189(+),1121(+)		1189(+), 1121(+)	ν_s(C—O—C) + ν_{as}(O—C—O), ν_s(CH_2—CH—CH_3)	PC
	1055(+)		1055(+)	ν_s(C—O)	ν_s(C—O)

[a]The band assignments were on the basis of refs 14, 34, and 37−41. [b]ν = stretching, τ = twisting, ζ = scissoring, δ = bending, ν_s = symmetric stretching, ν_{as} = asymmetric stretching ω = wagging [c](+) represent upward band indicating loss of species at the interface.

reported, both in PC and EC based electrolytes.[2,12,14,15,30−32] There have been several theoretical studies using quantum chemical methods, providing mechanistic insight into the ring opening reactions of cyclic carbonates in lithium ion batteries. It has been proposed that electron attack at the less hindered ethereal carbon is responsible for the solid electrolyte interphase (SEI) layer formation,[12,22,33] and a similar nucleophilic attack by superoxide species generated at the Li—O_2 cathode is believed to be responsible for the ring opening reactions of PC,[7,14,34] (Scheme 1). Furthermore, the effect of the Li-ion in the ring opening reaction has also been addressed using quantum chemical methods, and some of these studies indicated that the presence of Li^+ cation does not have a significant effect in the overall reaction in Li-ion battery environment.[20,35] As our SEIRAS studies of the PC-TEAClO$_4$ system indicate no major chemical change happening to PC at the interface in either oxygenated or deoxygenated environment, we extend our SEIRAS analysis to Li^+ ion containing PC electrolytes.

The voltammogram of the electrode in deoxygenated 0.1 M LiClO$_4$ containing PC shown in Figure 4 indicates the absence of any reversible redox reaction. Corresponding SEIRA spectra in Figure 5a also show only PC vibrational bands, but the intensity of the peaks and the shift of C═O stretch with potential is considerably lower when compared to the PC-TEAClO$_4$ system. This may indicate that the interaction of PC with the electrode surface is affected by the presence of Li^+ ions in the interfacial region. The cyclic voltammogram of oxygen reduction in PC-LiClO$_4$ is significantly different from the PC-TEAClO$_4$ system. A positive shift in the oxidation peak indicates that the presence of lithium influences the reversibility of oxygen reduction. As shown by previous authors, this peak can be related to the oxidation of solvent decomposition products.[14] In situ SEIRA analysis has been carried out to understand the superoxide induced changes to the interface relating to the difference in reversibility observed in the CVs.

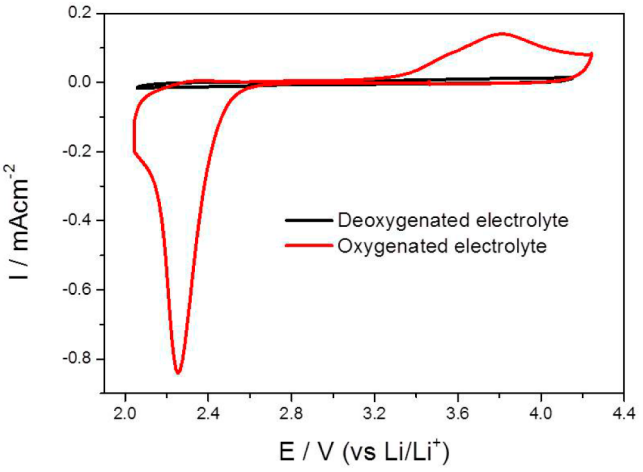

Figure 4. Cyclic voltammograms for the reduction of oxygen (red) and the argon background (black) in 0.1 M LiClO$_4$/PC, at 0.1 V/s scan rate.

Corresponding SEIRA spectra in Figure 5b show strong positive as well as negative bands as the electrode is negatively polarized (the same spectra over a broader range are provided in Figure S2). Upward going bands indicate the loss of PC at the interface, while strong downward bands indicate the formation of ring-opened carbonate species, $ROCO_2Li$. All the downward going bands appearing at the less positive potentials remain stable, even at the most anodic polarizations, indicating that the surface layer formed is relatively stable. SEIRAS bands for PC-LiClO$_4$ oxygenated as well as deoxygenated systems in the reduction as well as oxidation regions (2.12 and 3.7 V, respectively) are also summarized in

DOI: 10.1021/jacs.5b12494
J. Am. Chem. Soc. 2016, 138, 3745−3751

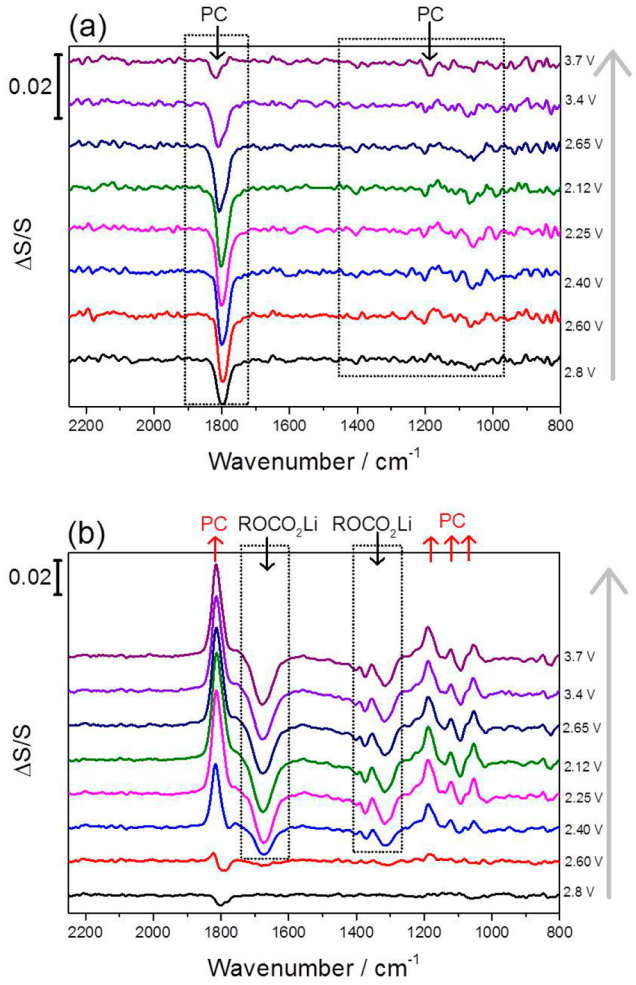

Figure 5. SEIRA spectra recorded for Au thin film electrode in deoxygenated 0.1 M $LiClO_4$/PC electrolyte at various representative electrode potentials. (a) Deoxygenated electrolyte—corresponds to the black CV curve in Figure 4, and (b) oxygen saturated electrolyte—corresponds to the red CV curve in Figure 4. The reference spectra were taken at the OCV (3.1 V) before the potential sweep started.

Table 1 (please also see Table S1). The PC ring-opened species observed here is in line with the surface film observed on Li—O_2 cathodes cycled in PC electrolyte.[14,34] Superoxide species generated during the reduction of oxygen at the cathode are believed to be responsible for this degradation reaction.[7,14,34] We have left a moderate downward going peak seen around 1094 cm^{-1} unassigned; this band may be related to a coordinated superoxide species,[36] but a detailed investigation is required before assigning this to superoxide because other species such as perchlorate also have infrared absorbance in this region.

Even though the reduction of molecular oxygen produces superoxide in both PC-$TEAClO_4$ and PC-$LiClO_4$ systems, interestingly there is no indication of a ring opened species in oxygenated PC-$TEAClO_4$ investigated here. This suggests that the presence of Li^+ cation is important in inducing the ring opening reaction of PC leading to significant surface film formation that eventually leads to Li—O_2 cell failure. We re-examined the behavior of oxygen reduction reaction on a Au electrode in PC-$LiClO_4$ by cyclic voltammetry at 0.1 V/s scan rate for an extended period (15 cycles) in a conventional three electrode cell. Representative cycles of this measurement shown in Figure 6a clearly demonstrate that the oxygen reduction peak has been greatly attenuated by the 15th cycle. We repeated the

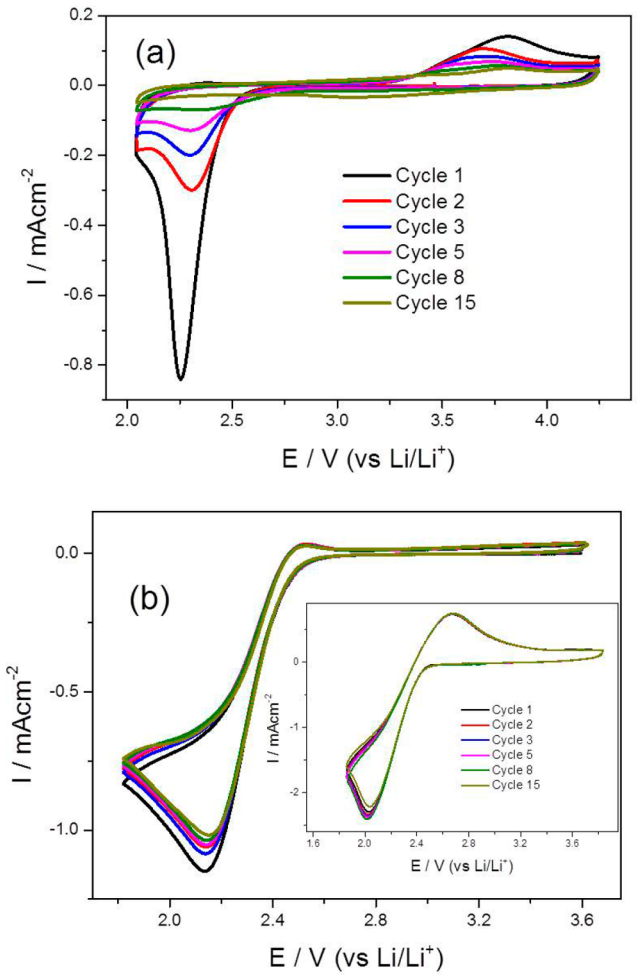

Figure 6. Representative voltammograms for extended oxygen reduction cycles in (a) 0.1 M $LiClO_4$/PC and (b) in 0.1 M $TEAClO_4$/PC, at 0.1 V/s scan rate. The inset of (b) shows oxygen reduction in $TEAClO_4$/PC, at 1 V/s scan rate.

same set of experiments in PC-$TEAClO_4$; the redox process is only slightly changed even after 15 cycles (Figure 6b). Voltammograms at a faster scan rate (1 V/s) shown in the inset of Figure 6b demonstrate the reversibility of the oxygen redox chemistry in TEA^+ even after several cycles. A comparison of the cyclic voltammograms of Li^+ and TEA^+ electrolytes clearly demonstrate that cationic species in the battery electrolyte plays a major role in the degradation of solvent at the interface. This understanding is particularly important for the development of electrolyte systems for Li—O_2 batteries.

Oxygen reduction in PC containing a larger alkali metal cation, Cs^+ also results in downward band at ~1670 cm^{-1} (Figure S3). This indicates that rather than the chemical nature or the size of the cationic species, the coordination of cations to the carbonyl group is significant in superoxide induced ring opening reactions of cyclic carbonate solvents. As bulky tetraalkylammonium cations cannot coordinate to the carbonyl group of PC because of steric hindrance, superoxide attack on the ethereal carbon is not favored in the PC-TEA^+ system. Additionally, some previous spectroscopic studies of lithium

DOI: 10.1021/jacs.5b12494
J. Am. Chem. Soc. 2016, 138, 3745−3751

oxygen cathode discharge in PC based electrolytes have shown lithium carbonate along with the ring opened lithium alkyl carbonates,[14,18] but we did not observe vibrational bands corresponding to Li_2CO_3 that would result from the further reaction of ring opened products of PC.

We have also looked at the generality of the superoxide induced ring opening in organic carbonate electrolytes by carrying out similar SEIRAS analysis of another popular battery electrolyte solvent EC. As shown in Figure S4, the SEIRA spectrum is similar to PC and shows a similar downward band that corresponds to the ring opened species after reaction with superoxide. This measurement was carried out at 40 °C in order for EC/0.1 M $LiClO_4$ to be in the liquid state. Unlike PC and EC, solvents like dimethyl sulfoxide (DMSO) are relatively stable in the presence of superoxide. A similar SEIRA analysis of DMSO under analogous conditions (i.e., oxygen reduction in the presence of Li^+) is also included in the SI (Figure S7); the spectra do not show any appreciable downward band other than the bands of DMSO, indicating that this solvent is relatively stable. The stability of DMSO/Li^+ in the oxygen reduction environment and the surface reactions probed in PC/Li^+ and EC/Li^+ electrolytes under the same conditions, can be related to the failure of Li—O_2 batteries in organic carbonate electrolytes and superior performance of Li—O_2 batteries when DMSO was used as the solvent.[3] Although the electrodes used in real Li—O_2 batteries would be different from the gold electrode used in our SEIRAS studies, the insights obtained through our approach are relevant because once superoxide has been generated its subsequent interaction with solvent molecules and cations is independent of the electrode substrate the superoxide was generated upon.

Computational studies using density function theory (M06-2x/6-311++(d,p)),[28,29] were performed on the reaction of superoxide with PC in the presence of Li^+ and TEA^+. The transition state for PC ring opening with Li^+ revealed two favorable interactions between oxygen atoms and the small, hard cation (Figure 7b) of 1.87 and 1.92 Å. There is no such coordination interaction observed between TEA^+ and the carbonate functionality (Figure 7c). This difference in coordination is presumably the major reason why a very large difference in activation energies was observed in the two reactions. The activation energy in the presence of Li^+ is 0.64 kcal/mol compared with 17.83 kcal/mol with TEA^+. This large difference in activation energy is consistent with the experimental findings.

In conclusion, we have demonstrated the effective use of ATR-SEIRAS technique in studying the interfacial processes relevant to the Li—O_2 battery system. The role of solvent coordinating cationic species in the degradation of PC solvent in an Li—O_2 environment has been investigated in this work, in which the presence of a PC coordinating Li^+ plays a significant role in lowering the activation barrier for superoxide induced ring opening reaction. Although our system does not account for a real battery/electrolyte interface; SEIRAS evaluation of battery electrolytes on model 2D noble metal electrodes has provided direct mechanistic insight into a significant reaction pathway and is thereby demonstrated as an important analytical approach for examining promising Li—O_2 battery electrolytes.

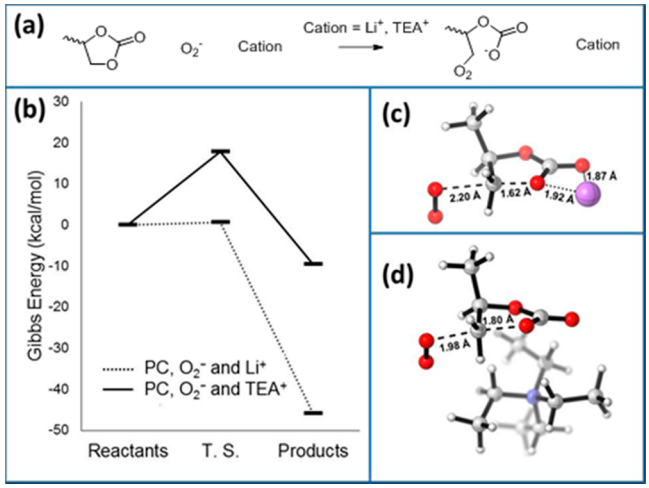

Figure 7. (a) Reaction modeled (b) energy profile and transition states for the reaction of PC with superoxide with Li^+ and TEA^+. Calculated structures of transition states with (c) Li^+ and (d) TEA^+ (carbon—gray, hydrogen—white, nitrogen—blue, oxygen—red, lithium—purple). Dashed lines represent the bonds being made and broken via the transition state. Dotted lines indicate coordinate bonds. Distances are stated in Å. Graphic generated using CylView (http://www.cylview.org/Home.html). Coordinates of reactants, transition states, and products can be found in the SI.

■ ASSOCIATED CONTENT

Supporting Information

The Supporting Information is available free of charge on the ACS Publications website at DOI: 10.1021/jacs.5b12494.

Seira spectra, ATR spectra, IR band assignments, electrochemical data, coordinates of reactants, transition states and products used in DFT calculations (PDF)

■ AUTHOR INFORMATION

Corresponding Author

*hardwick@liverpool.ac.uk

Notes

The authors declare no competing financial interest.

■ ACKNOWLEDGMENTS

We acknowledge the Engineering and Physical Sciences Research Council (EPSRC) for the funding of this research under Grant Number EP/K006835/1. The authors would like to thank Prof. Ken Durose (University of Liverpool) for the use of the thermal evaporator. G.P. acknowledges funding through the Marie Curie Innovative Training Network "NANO-EMBRACE".

■ REFERENCES

(1) Van Noorden, R. *Nature* **2014**, *507* (7490), 26−28.
(2) Bruce, P. G.; Freunberger, S. A.; Hardwick, L. J.; Tarascon, J.-M. *Nat. Mater.* **2011**, *11* (1), 19−29.
(3) Peng, Z.; Freunberger, S. A.; Chen, Y.; Bruce, P. G. *Science (Washington, DC, U. S.)* **2012**, *337* (6094), 563−566.
(4) Scrosati, B., Abraham, K. M., Van Schalkwijk, W., Hassoun, J., Eds. *Lithium Batteries*; John Wiley & Sons, Inc.: Hoboken, NJ, 2013.
(5) Luntz, A. C.; McCloskey, B. D. *Chem. Rev.* **2014**, *114* (23), 11721−11750.
(6) Girishkumar, G.; McCloskey, B.; Luntz, A. C.; Swanson, S.; Wilcke, W. *J. Phys. Chem. Lett.* **2010**, *1* (14), 2193−2203.

DOI: 10.1021/jacs.5b12494
J. Am. Chem. Soc. 2016, 138, 3745−3751

(7) Balaish, M.; Kraytsberg, A.; Ein-Eli, Y. *Phys. Chem. Chem. Phys.* **2014**, *16* (7), 2801−2822.
(8) Christensen, J.; Albertus, P.; Sanchez-Carrera, R. S.; Lohmann, T.; Kozinsky, B.; Liedtke, R.; Ahmed, J.; Kojic, A. *J. Electrochem. Soc.* **2012**, *159* (2), R1.
(9) Grande, L.; Paillard, E.; Hassoun, J.; Park, J.-B.; Lee, Y.-J.; Sun, Y.-K.; Passerini, S.; Scrosati, B. *Adv. Mater.* **2015**, *27* (5), 784−800.
(10) Xu, K. *Chem. Rev.* **2004**, *104* (10), 4303−4418.
(11) Xu, K. *Chem. Rev.* **2014**, *114* (23), 11503−11618.
(12) Haregewoin, A. M.; Leggesse, E. G.; Jiang, J.-C.; Wang, F.-M.; Hwang, B.-J.; Lin, S. D. *Electrochim. Acta* **2014**, *136*, 274−285.
(13) Aurbach, D.; Ein-Eli, Y.; Chusid, O.; Carmeli, Y.; Babai, M.; Yamin, H. *J. Electrochem. Soc.* **1994**, *141* (3), 603−611.
(14) Freunberger, S. A.; Chen, Y.; Peng, Z.; Griffin, J. M.; Hardwick, L. J.; Bardé, F.; Novák, P.; Bruce, P. G. *J. Am. Chem. Soc.* **2011**, *133* (20), 8040−8047.
(15) Tripachev, O. V.; Maleeva, E. A.; Tarasevich, M. R. *Russ. J. Electrochem.* **2015**, *51* (2), 103−111.
(16) Laoire, C. O.; Mukerjee, S.; Abraham, K. M.; Plichta, E. J.; Hendrickson, M. A. *J. Phys. Chem. C* **2010**, *114* (19), 9178−9186.
(17) Ottakam Thotiyl, M. M.; Freunberger, S. A.; Peng, Z.; Chen, Y.; Liu, Z.; Bruce, P. G. *Nat. Mater.* **2013**, *12* (11), 1050−1056.
(18) Zhang, T.; Zhou, H. *Nat. Commun.* **2013**, *4*, 1817.
(19) Adams, B. D.; Black, R.; Williams, Z.; Fernandes, R.; Cuisinier, M.; Berg, E. J.; Novak, P.; Murphy, G. K.; Nazar, L. F. *Adv. Energy Mater.* **2015**, *5* (1), 1400867.
(20) Wang, Y.; Nakamura, S.; Ue, M.; Balbuena, P. B. *J. Am. Chem. Soc.* **2001**, *123* (47), 11708−11718.
(21) Bryantsev, V. S.; Giordani, V.; Walker, W.; Blanco, M.; Zecevic, S.; Sasaki, K.; Uddin, J.; Addison, D.; Chase, G. V. *J. Phys. Chem. A* **2011**, *115* (44), 12399−12409.
(22) Coughlin, J. E.; Zhugayevych, A.; Bakus, R. C.; van der Poll, T. S.; Welch, G. C.; Teat, S. J.; Bazan, G. C.; Tretiak, S. *J. Phys. Chem. C* **2014**, *118* (29), 15610−15623.
(23) Mozhzhukhina, N.; Méndez De Leo, L. P.; Calvo, E. J. *J. Phys. Chem. C* **2013**, *117* (36), 18375−18380.
(24) Shi, F.; Ross, P. N.; Zhao, H.; Liu, G.; Somorjai, G. A.; Komvopoulos, K. *J. Am. Chem. Soc.* **2015**, *137* (9), 3181−3184.
(25) Osawa, M. *Bull. Chem. Soc. Jpn.* **1997**, *70* (12), 2861−2880.
(26) Heaps, D. A.; Griffiths, P. R. *Anal. Chem.* **2005**, *77* (18), 5965−5972.
(27) Futamata, M. *J. Phys. Chem. B* **2001**, *105* (29), 6933−6942.
(28) Frisch, M. J.; Trucks, G. W.; Schlegel, H. B.; Scuseria, G. E.; Robb, M. A.; Cheeseman, J. R.; Scalmani, G.; Barone, V.; Mennucci, B.; Petersson, G. A.; Nakatsuji, H.; Caricato, M.; Li, X.; Hratchian, H. P.; Izmaylov, A. F.; Bloino, J.; Zheng, G.; Sonnenberg, J. L.; Hada, M.; Ehara, M.; Toyota, K.; Fukuda, R.; Hasegawa, J.; Ishida, M.; Nakajima, T.; Honda, Y.; Kitao, O.; Nakai, H.; Vreven, T.; Montgomery, J. A., Jr.; Peralta, J. E.; Ogliaro, F.; Bearpark, M.; Heyd, J. J.; Brothers, E.; Kudin, K. N.; Staroverov, V. N.; Kobayashi, R.; Normand, J.; Raghavachari, K.; Rendell, A.; Burant, J. C.; Iyengar, S. S.; Tomasi, J.; Cossi, M.; Rega, N.; Millam, J. M.; Klene, M.; Knox, J. E.; Cross, J. B.; Bakken, V.; Adamo, C.; Jaramillo, J.; Gomperts, R.; Stratmann, R. E.; Yazyev, O.; Austin, A. J.; Cammi, R.; Pomelli, C.; Ochterski, J. W.; Martin, R. L.; Morokuma, K.; Zakrzewski, V. G.; Voth, G. A.; Salvador, P.; Dannenberg, J. J.; Dapprich, S.; Daniels, A. D.; Farkas, O.; Foresman, J. B.; Ortiz, J. V.; Cioslowski, J.; Fox, D. J. *Gaussian 09*, revision B.01; Gaussian, Inc.: Wallingford, CT, 2009.
(29) Zhao, Y.; Truhlar, D. G. *Theor. Chem. Acc.* **2008**, *120* (1−3), 215−241.
(30) Shkrob, I. A.; Zhu, Y.; Marin, T. W.; Abraham, D. *J. Phys. Chem. C* **2013**, *117* (38), 19255−19269.
(31) Veith, G. M.; Dudney, N. J.; Howe, J.; Nanda, J. *J. Phys. Chem. C* **2011**, *115* (29), 14325−14333.
(32) Baddour-hadjean, R.; Pereira-Ramos, J.-P. *Chem. Rev.* **2010**, *110*, 1278−1319.
(33) Wang, Y.; Balbuena, P. B. *J. Phys. Chem. B* **2002**, *106* (17), 4486−4495.
(34) Haregewoin, A. M.; Leggesse, E. G.; Jiang, J.-C.; Wang, F.-M.; Hwang, B.-J.; Lin, S. D. *J. Power Sources* **2013**, *244*, 318−327.
(35) Vollmer, J. M.; Curtiss, L. A.; Vissers, D. R.; Amine, K. *J. Electrochem. Soc.* **2004**, *151* (1), A178−A183.
(36) Janik, I.; Tripathi, G. N. R. *J. Chem. Phys.* **2013**, *139* (1), 014302.
(37) de Beer, W. H. J.; Heyns, A. M. *Spectrochim. Acta Part A Mol. Spectrosc.* **1981**, *37* (12), 1099−1107.
(38) Aurbach, D. *J. Electrochem. Soc.* **1993**, *140* (11), L155.
(39) Ikezawa, Y.; Ariga, T. *Electrochim. Acta* **2007**, *52* (7), 2710−2715.
(40) Pyun, S.-I. *Fresenius' J. Anal. Chem.* **1999**, *363* (1), 38−45.
(41) Zeegers-Huyskens, T.; Bator, G. *Vib. Spectrosc.* **1996**, *13* (1), 41−49.

DOI: 10.1021/jacs.5b12494
J. Am. Chem. Soc. 2016, 138, 3745−3751